Published in Optical Engineering 34, issue 8, 2377-2383, 1995
which should be used for any reference to this work


# High-carrier-frequency fan-out gratings fabricated by total internal reflection holographic lithography

**Peter Ehbets,** MEMBER SPIE
**Hans Peter Herzig**
**Markku Kuittinen***
University of Neuchâtel
Institute of Microtechnology
Rue Breguet 2
CH-2000 Neuchâtel, Switzerland
E-mail: ehbets@imt.unine.ch

**Francis S. M. Clube**
**Yves Darbellay**
Holtronic Technologies SA
Champs-Montant 12B
CH-2074 Marin, Switzerland

**Abstract.** Total internal reflection (TIR) holographic lithography is applied to the fabrication of binary diffractive optical elements with submicrometer surface relief features. The recording conditions for the intermediate TIR volume hologram, used for high-resolution proximity printing, are discussed. In particular, the fabrication of efficient high-carrier-frequency fan-out gratings is considered and experimental results are presented for an off-axis $9 \times 1$ fan-out element in photoresist with a carrier frequency of 1000 lines/mm.

*Subject terms: lithography; holography; gratings; optical interconnects.*

## 1 Introduction

Fan-out elements split an incoming beam into a regular array of equally intense beams.[1] They are key components for optical interconnects, and off-axis elements, in particular, are of interest for the realization of integrated planar micro-optical systems.[2] In this paper, the fabrication of efficient binary off-axis fan-out gratings for visible and near-IR light is investigated. This is a challenging task, because it requires a fabrication process with submicrometer resolution and also with high position accuracy over the entire surface of the diffractive optical element (DOE).

Highly efficient off-axis fan-out elements can be fabricated by holographic recording in dichromated gelatin or photopolymer.[3] In this case, volume diffraction in the thick grating structure enables high diffraction efficiency for incidence at the Bragg angle. Unfortunately, the high angular selectivity of volume holograms limits the useful numerical aperture at readout. Recently, the design of synthetic Bragg holograms with a binary surface relief has been proposed.[4–6] The modulated binary relief function of these elements is interesting because it can be realized in stable substrate materials with a single lithographic step. In addition, the angular selectivity is reduced compared to volume holograms. However, Bragg diffraction behavior and high first-order diffraction efficiency with thin binary phase gratings requires carrier grating periods of the order of the wavelength. As a consequence, electromagnetic diffraction theory must be applied to determine the diffraction efficiency of the grating structure.

Synthetic Bragg DOEs with submicrometer carrier grating periods have been fabricated by using direct electron beam (e-beam) writing[4] and by two-beam holographic recording in photoresist with an optimized object beam.[7] For industrial fabrication, however, photolithography is more convenient. The accurate transfer of submicrometer features ($< 0.5$ μm) requires the use of advanced lithographic equipment, such as deep-UV, x-ray, or phase-shift lithography. In this context, total internal reflection (TIR) holographic lithography represents a very flexible alternative approach that offers the required resolution over a large printing area.[8–10] We have investigated for the first time the potential of this lithographic technology for the fabrication of binary DOEs with submicrometer features in the relief. The main potential problems associated with holographic recording methods arise from coherent noise and intermodulations that degrade the binary surface relief structure. The off-axis fan-out gratings considered are sensitive to fabrication errors. Therefore, the quality of the fabricated off-axis fan-out gratings provides a good criterion for the precision of the TIR holographic printing process.

TIR holographic lithography is a proximity copying technique and therefore requires a $1 \times$ amplitude mask of the final structure. In the following section, we present the encoding of the amplitude mask for high-carrier-frequency fan-out gratings. This high-resolution mask is then fabricated by e-beam writing. The influence of quantization errors on the

* On leave from University of Joensuu, Department of Physics, Väisälä Laboratory, P.O. Box 111, FIN-80101, Joensuu, Finland.

fan-out function is analyzed using rigorous electromagnetic diffraction theory. In the third section, the recording conditions of the intermediate TIR volume hologram for high reconstruction fidelity are discussed. Experimental results of holographically printed fan-out elements are then given in Sec. 4.

## 2 Encoding of Binary Off-Axis Fan-Out Gratings

The readout geometry of binary off-axis fan-out gratings in transmission is represented in Fig. 1. The grating structure is illuminated from the substrate of refractive index $n_s$ with a TE-polarized, monochromatic plane wave at the Bragg angle $\theta_B = \arcsin(\lambda/2n_s d_c)$, where $\lambda$ is the free-space wavelength and $d_c$ is the period of the carrier grating. The carrier grating is modulated so that it generates the desired fan-out function in the $-1$st diffraction order. For off-axis incidence, higher diffraction orders can be made evanescent by the use of a high carrier frequency. From the grating equation, it follows that only the zero and the $-1$st diffraction orders are propagating in the output medium ($n = 1$), if the carrier grating period is in the range $0.5\lambda < d_c < 1.5\lambda$. Rigorous analysis has shown that in this case, high $-1$st order diffraction efficiencies can be achieved for Bragg angle incidence and for an appropriate choice of the binary grating parameters.[5]

The modulated high-frequency grating structure for off-axis fan-out generation can be efficiently calculated using hybrid encoding schemes,[4–6] which assume a slowly varying modulation signal compared to the carrier frequency. In this case, the off-axis fan-out function can be described by the normalized interference function

$$I(x) = \frac{1}{2} + \frac{1}{2}\cos[2\pi x/d_c - \Phi(x)] \ , \tag{1}$$

where $\Phi(x)$ represents the phase function of an on-axis fan-out element, which can be determined by paraxial scalar diffraction theory. High fan-out efficiency $\eta_F$ is achieved by calculating an on-axis fan-out element $\Phi(x)$ with a continuous phase function using iterative Fourier optimization.[11] For 2-D

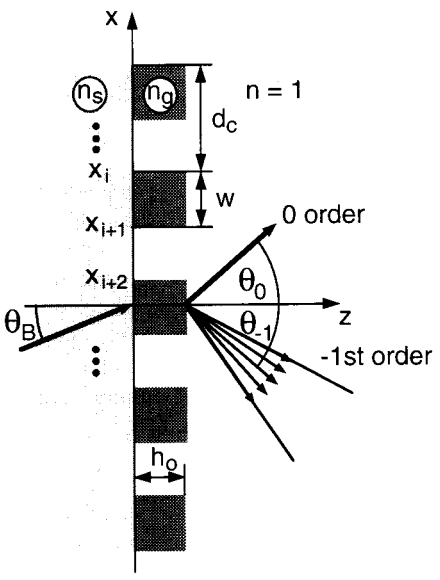


**Fig. 1** Readout geometry of high-carrier-frequency off-axis fan-out gratings in transmission.

elements, the strip geometry of Ref. 6 is advantageous for mask encoding.

The binary amplitude transmittance function $T(x)$ of the required mask is obtained from Eq. (1) by hard clipping the interference function $I(x)$ to 0 and 1, which can be written as

$$T(x) = \frac{1}{2} + \frac{1}{2}\,\mathrm{sign}\{\cos[2\pi x/d_c - \Phi(x)]\} \ , \tag{2}$$

where $\mathrm{sign}(x) = 1$ for $x > 0$ and $\mathrm{sign}(x) = -1$ for $x \le 0$. This results in a pulse-frequency-modulated carrier grating with a local filling factor ($f = w/d_c$) equal to $f \cong 0.5$. If the period $\Lambda$ of the fan-out function $\Phi(x)$ is an integer multiple of $d_c$, i.e., $\Lambda = Nd_c$, the overall period of $T(x)$ becomes equal to $\Lambda$ and is completely defined by $2N$ transition points $x_i$, determined from Eq. (2).

The final phase grating printed in positive photoresist is determined by the binary surface-relief function $h(x)$, which can then be written as

$$h(x) = h_0[1 - T(x)] \ , \tag{3}$$

where $h_0$ represents the relief depth. Because the carrier grating is locally only weakly perturbed, the efficiency in the $-1$st order can be optimized using rigorous diffraction theory by considering only the carrier grating.

The overall diffraction efficiency $\eta$ of the off-axis fan-out element is defined by the combined efficiency of the fan-out signal beams, which can be written as

$$\eta = \sum_{i=1}^{N} \eta_i \ , \tag{4}$$

where $\eta_i$ are the efficiencies of the $N$ fan-out diffraction orders. We can estimate the value of the diffraction efficiency $\eta$ in the hybrid encoding approach by calculating the hybrid diffraction efficiency $\eta_H$, which is determined by $\eta_H = \eta_{-1}\eta_F$, where $\eta_{-1}$ represents the $-1$st order efficiency of the carrier grating and $\eta_F$ is the efficiency of the paraxial fan-out element. The value of $\eta_F$ indicates the fraction of the power inside the $-1$st carrier grating order, which falls in the ideal case into the desired $N$ fan-out orders.

The quality of the encoded off-axis fan-out element is characterized by the uniformity error $u$, which can be defined by the contrast function

$$u = \frac{\eta_{\max} - \eta_{\min}}{\eta_{\max} + \eta_{\min}} \ , \tag{5}$$

where $\eta_{\max}$ and $\eta_{\min}$ are the maximum and minimum efficiencies of the fan-out diffraction orders $\eta_i$. The validity of the hybrid encoding approach and the conditions for high efficiency and low uniformity error are discussed in Ref. 5.

We encoded a $9 \times 1$ fan-out element of period $\Lambda = 125.0$ μm with a carrier frequency of 1000 lines/mm. The continuous phase function of the on-axis $9 \times 1$ fan-out element was optimized according to Ref. 11. It offers a high fan-out efficiency of $\eta_F = 99.3\%$ and a uniformity error below 0.1%. In this case, the carrier grating period of the amplitude transmittance function $T(x)$ in Eq. (2) varies continuously between 0.96 and 1.04 μm.

Fabrication of the amplitude mask by e-beam writing[12] requires quantization of the exact transition points $x_i$ to the pixel grid of the e-beam writer. For high resolution, typical pixel sizes are in the range of 25 to 100 nm. We used a pixel grid equal to $\Delta = 50$ nm, which corresponds to a scan field of $800 \times 800$ μm$^2$. For larger grating patterns, stitching of several scan fields must be applied, which introduces stitching errors between the fields of the order of 100 nm. The encoded solution was obtained by rounding the exact transition points $x_i$ to the nearest grid position. The rounding of the transition points shifts the centers of the binary grating pulses and introduces detour phase errors in the fan-out phase function $\Phi(x)$ up to $\pi\Delta/d_c = \pi/20$. In addition, rounding introduces fast modulation on the carrier grating period $d_c$ of the order of $\Delta$ and also modulates the filling factor. This results in additional amplitude modulation of the emerging wavefront in the −1st diffraction order. Detour phase errors and amplitude modulation will deteriorate the uniformity of the array.

The performance of the encoded amplitude mask was first evaluated using amplitude transmittance theory and scalar wave propagation. In this approximation, ideal transition points would still produce a uniformity error below 1%, whereas the solution with rounded transition points yields a uniformity error $u = 3\%$. This increase is essentially caused by the detour phase errors. Rigorous diffraction theory was applied to analyze the diffraction efficiency and the uniformity of the high-carrier-frequency surface-relief fan-out gratings in photoresist. An efficient implementation for rigorous analysis of dielectric gratings has been obtained by using Knop's model,[13] as described in Refs. 5 and 14. We considered readout with a TE-polarized HeNe laser of wavelength $\lambda = 633$ nm at the Bragg angle, as shown in Fig. 1. Refractive indices of $n_s = 1.515$ for the BK7 glass substrate and $n_g = 1.645$ for the photoresist are assumed. In this geometry, two additional carrier grating diffraction orders, the +1st and −2nd orders, are below cutoff in the air region and in the substrate region. The evolution of the diffraction efficiency $\eta$ in the fan-out orders and the uniformity error $u$ as a function of the relief depth $h_0$ are shown in Fig. 2. The continuous curve represents the hybrid efficiency $\eta_H = \eta_{-1}\eta_F$, where only the −1st order carrier grating efficiency $\eta_{-1}$ is rigorously calculated and $\eta_F$ represents the efficiency of the on-axis fan-out solution. The markers represent rigorously calculated values for the efficiency $\eta$ (x markers) and the uniformity error $u$ (o markers) of the modulated carrier grating structure of period $\Lambda = 125.0$ μm. The results for the modulated carrier grating with large paraxial periodicity were obtained by considering about 900 orders in the expansions that describe the diffracted electromagnetic fields.[13] This value was limited by the available memory space for the computation. In this case, the diffraction orders up to the first two evanescent orders of the carrier grating on both sides of the propagating orders are retained in the analysis. Convergence of the results were verified for smaller fan-out periods $\Lambda$, where more evanescent orders can be included. It is seen that the hybrid efficiency $\eta_H$ is a good approximation of the rigorously calculated efficiency $\eta$, even in the case of a large uniformity error. In the region of maximum efficiency, around $h_0 = 1.2$ μm, however, the hybrid calculation gives slightly too high values for the efficiency. Low uniformity errors, comparable to the 3% predicted by scalar theory, are obtained for small relief depths $h_0 \leq 0.4$ μm. For deeper gratings, the uniformity error increases up to 40% and the hybrid encoded solution fails. It was found that in this region of low efficiency, the −1st order efficiency of the carrier grating depends strongly on the variations of the carrier grating period $d_c$. Therefore, the fast frequency modulation of the rounded solution introduces considerable amplitude modulation, which becomes more important than the detour phase errors. In the region of interest with high efficiency around $h = 1.2$ μm, again a low uniformity error in the order of $u = 5\%$ is reached. In this region the −1st order efficiency is stable against variation of the carrier grating period and the filling factor, and the uniformity error is essentially determined by the detour phase errors.

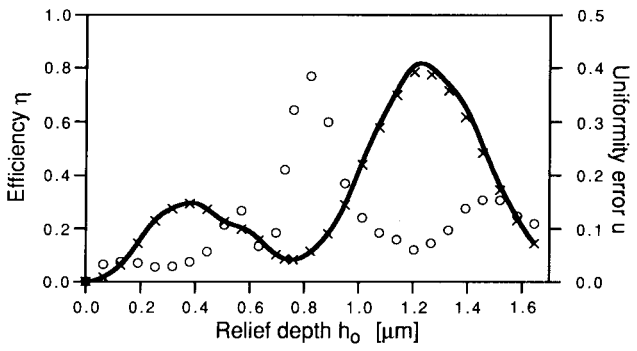


**Fig. 2** Performance of the high-carrier-frequency fan-out gratings in photoresist as a function of relief depth $h_0$: solid line, calculated efficiency $\eta_H$ in the hybrid approach; x markers, rigorously calculated efficiency $\eta$ of the modulated carrier grating; and o markers, rigorously calculated uniformity error $u$ of the modulated carrier grating.

## 3 TIR Holographic Lithography

A commercially available holographic mask aligner (HMA 150) was used to copy the high-resolution fan-out mask into photoresist. A detailed description of this system, which is able to print features down to 0.25 μm over substrates up to 6- × 6-in., is given in Refs. 10 and 15. The principle of this holographic mask aligner is based on TIR near-field holography, which is able to print submicrometer features.[8,9] The recording geometry of the intermediate TIR volume hologram is shown in Fig. 3. The chrome mask is placed near the holographic layer, typically at a distance of $d_g = 100$ μm. The mask is then illuminated with a collimated expanded beam, which is polarized perpendicularly to the plane of incidence (TE). The diffracted field from the mask interferes in the holographic layer with the reference wave at 45-deg incidence, which is fed through a prism and totally internally reflected at the film-air interface. The resulting interference pattern consists of three primary grating structures: a reflection grating from the interference of the object beam with the reference wave, a transmission grating from the interference of the object beam with the TIR wave, and a Lippmann grating from the interference of the reference wave with the TIR wave. In addition, the self-interference of the object beam in the holographic layer produces undesired intermodulation gratings.

At readout, the TIR hologram is illuminated with the conjugate reference beam at the recording angle. Interaction with mainly the transmission grating generates the conjugate of the recorded object beam, which reconstructs the original

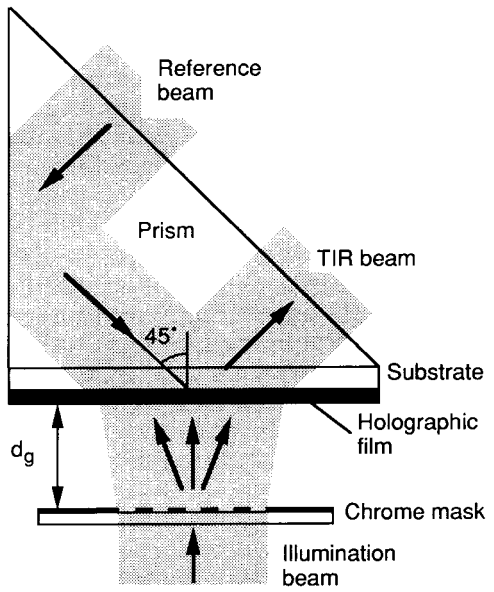


**Fig. 3** Recording geometry of the intermediate volume hologram for TIR holographic lithography.

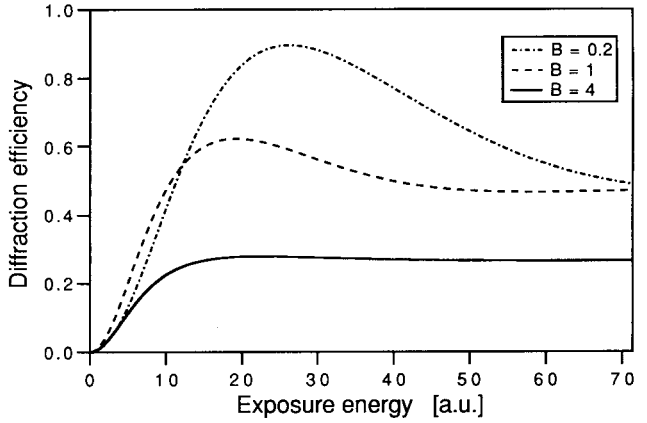


**Fig. 4** Diffraction efficiency of the TIR volume hologram versus exposure energy calculated for TE polarization and for different recording reference-to-object beam ratios: $B=0.2$, 1, and 4.

mask pattern at the distance $d_g$. For lithographic applications, the critical process parameters are high reconstruction fidelity and low coherent noise. This requires that all the recorded primary gratings are optically thick and generate only one diffraction order. For the recording of object beams with high numerical apertures, this condition can be satisfied by increasing either the thickness of the holographic layer or the recording angle of the reference beam. Undiffracted light in the reference beam is backreflected because of the TIR condition and cannot reach the printing area. Intermodulation effects are minimized for a high reference-to-object beam ratio at recording. This produces a strong Lippmann grating that couples light directly from the reference wave to the TIR wave. In a previous publication,[16] we analyzed the diffraction behavior of TIR holograms recorded with plane waves by using a model based on first-order coupled wave theory. We used this model and studied the diffraction efficiency in the object beam as a function of the exposure energy for different reference-to-object beam ratios $B$. The results are represented in Fig. 4. For the calculation, a linear relation between the index modulation and the exposure energy was assumed. For small beam ratios of $B<1$, high diffraction efficiency in the object beam is possible. If the beam ratio is increased, the diffraction efficiency saturates before high values are reached. The typical sinusoidal diffraction efficiency characteristic of a single thick phase grating in transmission is no longer observed. As a consequence, the high recording beam ratio required for high reconstruction fidelity affects the diffraction efficiency in the TIR geometry.

The Lippmann grating can be eliminated by the use of TM-polarized light at recording, because then the electric field vectors of the reference wave and the TIR wave are orthogonal. However, for TM-polarized light the index modulation of the grating depends on the angle between the two recording beams.[17] This results not only in a smaller contrast compared to TE polarization but also, because of the off-axis incidence of the reference beam, in an asymmetric angular attenuation of the transmission grating index modulation. The consequence is a reduction of the contrast in the image plane at readout, therefore the use of TE polarization is preferable for printing high-resolution features.

The intermediate TIR volume hologram of the fan-out mask was recorded in a 15-μm-thick layer of the photopolymer material (HRS 352 without dye) from Du Pont[18] using an argon laser at $\lambda=363.8$ nm. The final elements are printed into a layer of *g/i*-line resist (O.C.G. HiPR 6512), which is compatible with the UV argon laser wavelength. To ensure uniform illumination of the photoresist layer over the printing area, the TIR volume hologram was scanned at readout. Standard resist processing according to the manufacturer was used for the preparation of the plates and the development.

## 4 Experimental Results

The off-axis $9\times1$ fan-out elements were printed by TIR holographic lithography into photoresist on silicon wafers and on glass substrates. The silicon wafers were used for scanning electron microscope (SEM) inspection of the resulting photoresist relief, carried out by first coating the relief with a thin gold layer. Figures 5(a) and 5(b) show cross-sectional and top views of the fabricated modulated grating structure with a carrier grating period of $d_c=1.0$ μm. A binary relief with almost vertical sidewalls and a filling factor of $f=0.5$ can be seen. The small ripples in the sidewalls result from standing wave patterns in the resist layer at recording. These effects are reduced for the gratings recorded on the glass substrate with an absorber on the back side because of the smaller reflectivity of the glass substrates compared to the silicon wafers. The uniform relief depth of about 1.0 μm indicates that, using the recording conditions for the TIR hologram described in the previous section, an accurate transfer of the mask pattern into a deep binary grating structure can be achieved.

The elements on the glass substrates were optically characterized. The relief depth of the grating structure was determined to be $h\cong1.15$ μm by measuring the thickness of the photoresist layer at a large opening in resist near the grating region with a mechanical stylus. We measured the efficiency of the $9\times1$ fan-out signal in the $-1$st transmission order

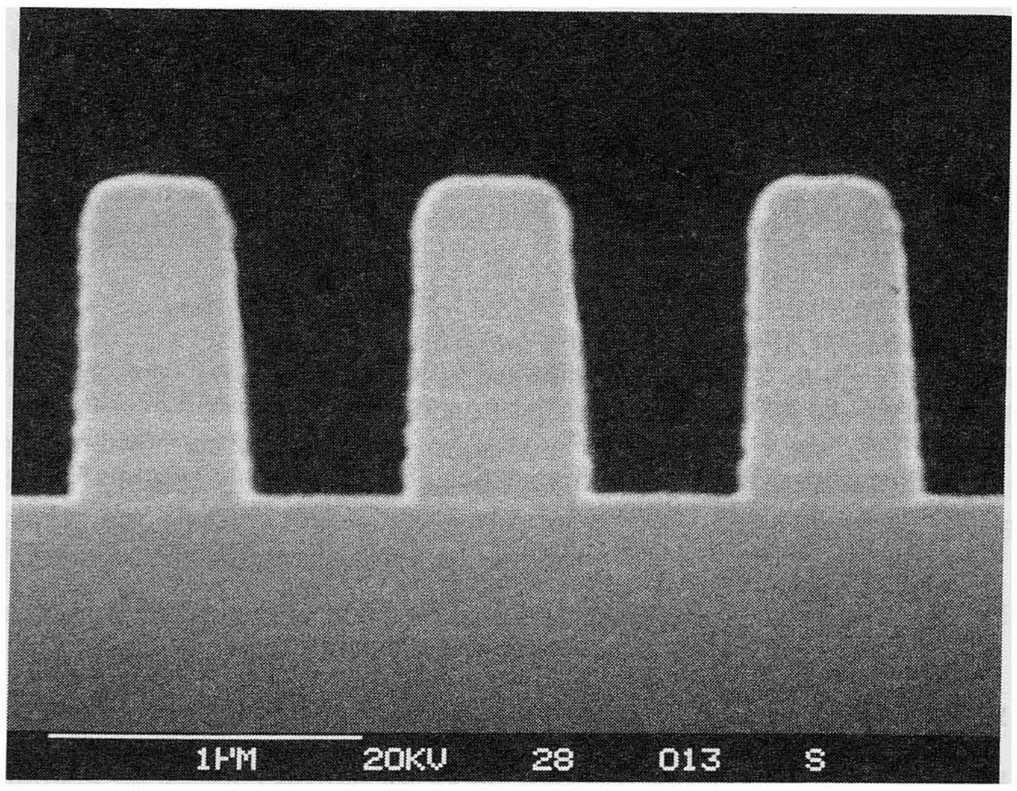


(a)

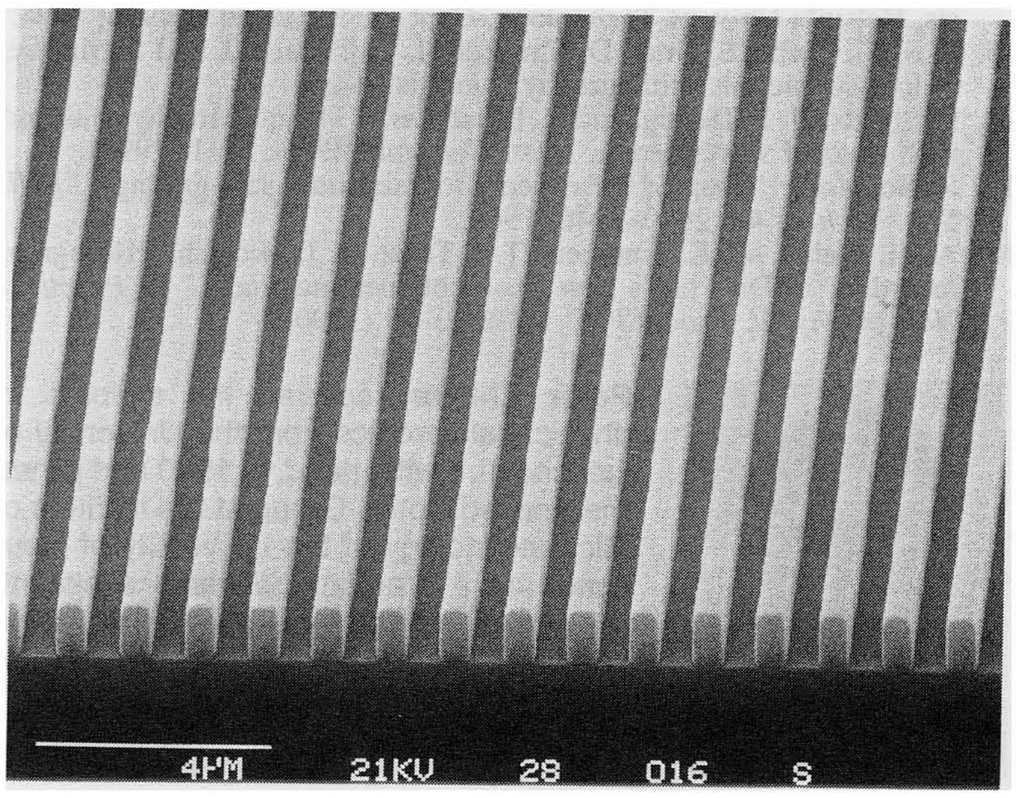


(b)

**Fig. 5** SEM pictures of the fabricated modulated high-carrier-frequency surface relief grating in photoresist: (a) cross-section view of the relief profile and (b) top view on a larger scale.

over the near-IR region, where the grating reaches its maximum efficiency. As a light source for the measurement, we used a tunable titanium-sapphire laser. The measurements were made with TE-polarized light for Bragg angle incidence from air to the grating medium. A wedge was index matched at the back side of the substrate, to eliminate fluctuations of the diffraction efficiency resulting from Fabry-Pérot effects in the substrate. Figure 6 represents the measured values (o markers) with error bars. Fresnel reflection losses at the wedge-air interface were compensated. A maximum efficiency of $\eta \approx 77\%$ is obtained for a wavelength of $\lambda = 830$ nm. For comparison, we also plotted the rigorously calculated efficiency $\eta$ of the modulated grating (x markers) and the hybrid efficiency $\eta_H$ (solid line), as described in Sec. 2. For the calculation, refractive index dispersion curves for the BK7 glass substrate and for the photoresist are taken from the manufacturers data sheets. Good agreement between the measured efficiency and the rigorously calculated values is obtained. The high diffraction efficiencies near 90% in the region of $\lambda = 860$ nm and the pronounced decrease predicted by the hybrid efficiency calculation are not observed in measurements. The measured behavior, however, is confirmed by the rigorous calculation of the modulated structure and can be explained by the fact that in this region, the $-1$st order efficiency of the carrier grating is sensitive to frequency modulation. The differences of the measurements compared to theory of the order of 5% are caused by scattering losses, absorption in the photoresist, and deviations from the ideal relief parameters, which are not considered in the theoretical model.

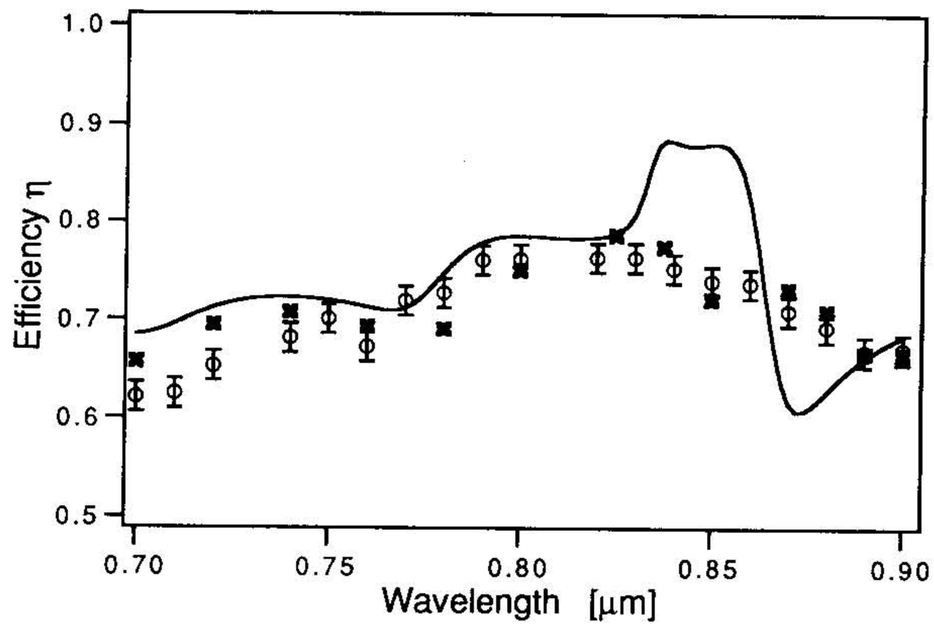


**Fig. 6** Fan-out efficiency as a function of the readout wavelength for TE polarization: o markers, measured efficiency values with mean error; x markers, rigorously calculated efficiency $\eta$ of the modulated carrier grating; and solid line, calculated hybrid efficiency $\eta_H$ of the carrier grating.

The uniformity of the fan-out elements was characterized using a HeNe laser at $\lambda = 632.8$ nm. The measurements were made by scanning with a detector through the spot array in the back focal plane of a lens for incidence from the substrate to air with TE polarization. Therefore, they can be directly compared to the calculated encoding errors in Sec. 2. At this wavelength, we measured a diffraction efficiency of about 70%, which corresponds to the rigorous value calculated in Fig. 2. To determine the quality of the TIR holographic lithographic process, we analyzed the fan-out function of the original amplitude mask and the copy in photoresist. Minimum uniformity errors are found, when one scan field ($800 \times 800\ \mu m^2$) of the e-beam writer is illuminated. In this case, about six periods of the fan-out function are illuminated and small random positioning errors inside the scan field are averaged. The amplitude mask produces uniformity errors of the order of 5%, which are only slightly higher than the predicted value of 3% by scalar theory. The binary surface relief grating in photoresist generates larger uniformity errors of about 9%. However, uniformity errors of this size are predicted by the rigorous analysis shown in Fig. 2 for a relief depth of $h = 1.15\ \mu m$. Therefore, they were not introduced during the TIR holographic printing. Figure 7 shows an intensity line scan through the array generated by the off-axis fan-out elements in the photoresist. If more than one scan field is illuminated, the uniformity error of both elements fluctuates strongly, depending on the position of the element. In this case, larger stitching errors between the scan fields degrade the performance. If the whole element ($10 \times 10\ mm^2$) is illuminated, the amplitude mask and the element copied

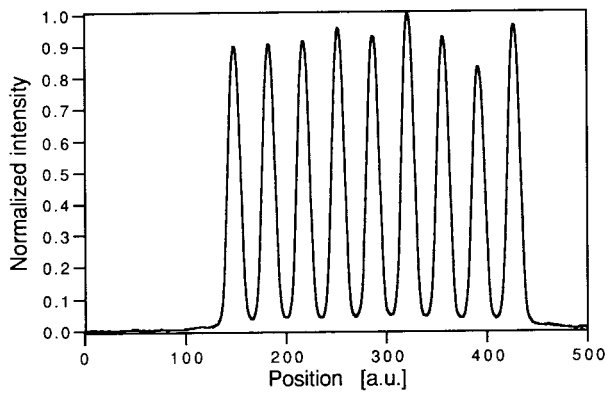


**Fig. 7** Measured far-field intensity distribution of the 9×1 fan-out diffraction orders.

in photoresist generate again a fan-out with good uniformity: 6% uniformity error for the mask and 10% for the copy.

## 5 Conclusions

Off-axis fan-out gratings with a carrier grating frequency equal to 1000 lines/mm were fabricated using an unconventional lithographic approach, based on TIR holography. In a single holographic printing exposure, rectangular grating shapes with deep relief depths up to 1.15 μm were achieved in photoresist, which resulted in fan-out efficiencies close to 80% in transmission for near-IR light. Optical characterization of the fabricated elements showed that the measured efficiency and uniformity is close to the ideal performance of the encoded element over the printed area of 1 $cm^2$. The fabrication process is not yet limited by the resolution of the photolithographic step, so that the printing of even smaller period grating structures with good optical quality and over much larger areas is realizable. The results demonstrate clearly that TIR holographic lithography is able to provide high-quality, binary DOEs with submicrometer surface relief features. It is therefore an interesting solution for the fabrication of a broad range of high-resolution elements, including grating couplers, off-axis lenses, and Dammann gratings with large diffraction angles.

### *Acknowledgments*

The authors would like to thank J. Turunen for helpful discussions on rigorous diffraction calculations. This work was partially supported by the Swiss Priority Program, Optique, and by the CERS (Commission pour l'Encouragement de la Recherche Scientifique). M. Kuittinen acknowledges the Academy of Finland and the Finnish Academy of Science for financial support.

### *References*

1. N. Streibl, "Beam shaping with optical array generators," *J. Mod. Opt.* **36** 1559–1573 (1990).
2. D. Prongué and H. P. Herzig, "Total internal reflection holography for optical interconnections," *Opt. Eng.* **33**(2), 636–642 (1994).
3. B. Robertson, J. Turunen, H. Ichikawa, J. M. Miller, M. R. Tagizadeh, and A. Vasara, "Hybrid kinoform fanout holograms in dichromated gelatin," *Appl. Opt.* **30,** 3711–3720 (1991).
4. J. Turunen, P. Blair, J. M. Miller, M. R. Tagizadeh, and E. Noponen, "Bragg holograms with binary surface-relief profile," *Opt. Lett.* **18,** 1022–1024 (1993).
5. E. Noponen and J. Turunen, "Binary high-frequency-carrier diffractive optical elements: electromagnetic theory," *J. Opt. Soc. Am. A* **11,** 1097–1109 (1994).
6. E. Tervonen, J. Turunen, and J. Pekola, "Pulse-frequency-modulated high-frequency-carrier diffractive elements for pattern projection," *Opt. Eng.* **33**(8), 2579–2587 (1994).
7. P. Ehbets, H. P. Herzig, P. Nussbaum, P. Blattner, and R. Dändliker, "Interferometric fabrication of modulated submicron gratings in photoresist," *Apl. Opt.* (in press) (1995).
8. R. Dändliker and J. Brook, "Holographic photolithography for submicron VLSI structures," in *Holographic Systems, Components and Applications,* Conference Publication Number **311,** pp. 127–132, Institution of Electrical Engineers, London (1989).
9. R. T. Chen, L. Sadovnik, T. M. Aye, and T. Jannson, "Submicron lithography using lensless high-efficiency holographic systems," *Opt. Lett.* **15,** 868–871 (1990).
10. F. Clube, S. Gray, D. Struchen, J. C. Tisserand, "Holographic mask aligner," *Opt. Eng.* **32**(10), 2403–2409 (1993).
11. H. P. Herzig, D. Prongué, and R. Dändliker, "Optimized kinoform structures for highly efficient fan-out elements," *Jpn. J. Appl. Phys.* **27,** 1307–1309 (1990).
12. M. J. Verheijen, "E-beam lithography for digital holograms," *J. Mod. Opt.* **40**(4), 711–721 (1993).
13. K. Knop, "Rigorous diffraction theory for transmission phase gratings with deep rectangular grooves," *J. Opt. Soc. Am.* **68,** 1206–1210 (1978).
14. E. Noponen, "Electromagnetic theory of diffractive optics," PhD. Thesis, Helsinki Univ. of Technology, Dept. of Technical Physics, 1994.
15. F. S. M. Clube, S. Gray, D. Struchen, J. C. Tisserand, and S. Malfoy, "Holographic microlithography," in this issue.
16. P. Ehbets, H. P. Herzig, and R. Dändliker, "TIR holography analyzed with coupled wave theory," *Opt. Commun.* **89**(1), 5–11 (1992).
17. H. Kogelnik, "Coupled wave theory for thick hologram gratings," *Bell. Syst. Tech. J.* **48,** 2909–2946 (1969).
18. A. M. Weber, W. K. Smothers, T. J. Trout, D. J. Mickish, "Hologram recording in Du Pont's new photopolymer materials," in *Practical Holography IV, Proc. SPIE,* **1212,** 30–39 (1990).

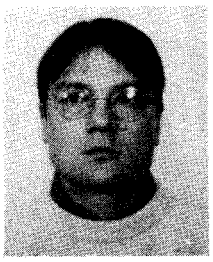

**Peter Ehbets** received the diploma in physical electronics from the University of Neuchâtel, Switzerland, in 1990 and joined the Applied Optics Group at the Institute of Microtechnology of the University of Neuchâtel as a graduate research assistant. His current research deals with the design and fabrication of diffractive optical elements for beam shaping and optical interconnects.

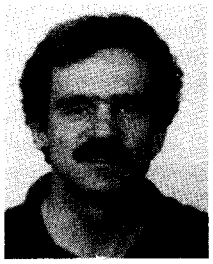

**Hans Peter Herzig** received the diploma in physics from the Swiss Federal Institute of Technology in Zürich (ETHZ), Switzerland, in 1978. From 1978 to 1982 he was a scientist in the Optics Development Department of the Kern Company in Aarau, Switzerland, where he worked in lens design and optical testing. In 1983, he joined the Applied Optics Group at the Institute of Microtechnology of the University of Neuchâtel, Switzerland, as a graduate research assistant, working in the field of holographic optical elements, especially scanning elements. In 1987, he received the PhD degree in optics from the University of Neuchâtel. Currently, he is lecturing modern optics and is responsible for the research in micro-optics, including diffractive optical elements and microlenses.

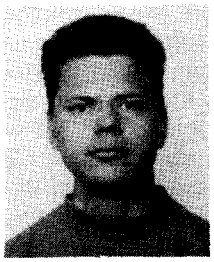

**Markku Kuittinen** received the MS and LicPhil degrees in physics from the University of Kuopio in 1989 and 1992, respectively, and the PhD degree in physics from the University of Joensuu in 1994, where he is a research assistant in the Department of Physics. Currently he is a visiting researcher at the Institute of Microtechnology in Neuchâtel, Switzerland. His research interests are in the area of numerical simulation and design and optimization of diffractive optical elements.

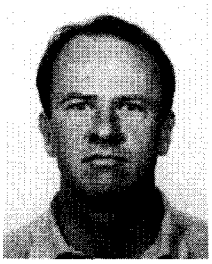

**Francis S. M. Clube** studied physics at Oxford University, graduating in 1981. He then spent eight years at the GEC-Marconi Research Centre working on a variety of holographic projects, including work on the development of the LANTIRN head-up display (HUD) for the F16 aircraft, the world's first holographic HUD to be put into production. Thereafter he was in charge of the holographic development program for a more advanced HUD, which has since been selected for the new European Fighter Aircraft. Mr. Clube joined Holtronic Technologies in 1989, where he developed the fine alignment system and is now the company's chief scientist. He is the author of several patent applications.

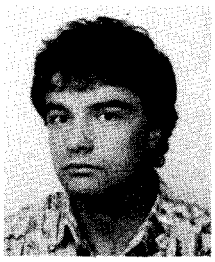

**Yves Darbellay** obtained his engineering degree in microtechnology from the Swiss Federal Institute of Technology, Lausanne, in 1993. He is now with Holtronic Technologies as an optical engineer in the production of large holographic masks.